

Article

Low-Temperature, Solution-Processed, Transparent Zinc Oxide-Based Thin-Film Transistors for Sensing Various Solvents

Hsin-Chiang You * and Cheng-Jyun Wang

Department of Electronic Engineering, National Chin-Yi University of Technology, No. 57, Section 2, Zhongshan Road, Taiping District, Taichung 41170, Taiwan; eddie415004@gmail.com

* Correspondence: hcyou@ncut.edu.tw; Tel.: +886-937-250-493

Academic Editor: Dirk Lehmkus

Received: 28 July 2016; Accepted: 22 February 2017; Published: 26 February 2017

Abstract: A low temperature solution-processed thin-film transistor (TFT) using zinc oxide (ZnO) film as an exposed sensing semiconductor channel was fabricated to detect and identify various solution solvents. The TFT devices would offer applications for low-cost, rapid and highly compatible water-soluble detection and could replace conventional silicon field effect transistors (FETs) as bio-sensors. In this work, we demonstrate the utility of the TFT ZnO channel to sense various liquids, such as polar solvents (ethanol), non-polar solvents (toluene) and deionized (DI) water, which were dropped and adsorbed onto the channel. It is discussed how different dielectric constants of polar/non-polar solvents and DI water were associated with various charge transport properties, demonstrating the main detection mechanisms of the thin-film transistor.

Keywords: thin-film transistor (TFT); zinc oxide (ZnO); bio-sensor; transparent conducting oxide (TCO); polar solvent

1. Introduction

In recent years, great progress has been made in biotechnology electronic devices which are a great aid in human health and longevity research. Fluorescence techniques have been mainly used for detecting biological diseases traditionally, but the detecting procedure is time-consuming and expensive. Among bio-electronic devices, thin-film transistors (TFTs) have much promise as novel tools to study biochemical interactions. They may be used in sophisticated medical devices as well as disposable electronic devices. Due to the maturation of TFT fabrication technology, small-size TFTs can be integrated into high-density TFT arrays for direct, rapid, and inexpensive medical diagnosis. Moreover, TFTs are based on transparent conducting oxide (TCO) materials and can be fabricated by solution-process based technique, showing some advantages of low cost and low-processing temperature and compatibility with flexible substrates [1–4]. Solution-processed semiconductors have been intensively investigated for use in large-area flexible sol-gel fabrication and electronic device inkjet-printing [5–8]. However, it has remained a challenge to achieve high performance and stability of oxide semiconductors using low-temperature process in the range of 200 and 300 °C which is needed for flexible substrates. These substrates are especially interesting for biological applications and enable the use of a wide range of biocompatible and biodegradable materials and devices, including bio-inspired peptide nanostructures [9], 2D nanostructuring of biosensor with nanodiamonds [10], ion-sensitive electrochemical transistors [11], pH sensors [12–14], and various label-free biosensing thin-film transistors [15–18].

Herein, we report the design, evaluation and fabrication of solution-processed ZnO-based TFTs by low-temperature processing and some effects of polar and non-polar liquid solvents on the exposed ZnO channel.

2. Materials and Experimental Section

Figure 1a presents the structure diagram of a zinc oxide based thin-film transistor (ZnO-based TFT) which is composed of bottom gate electrode, p-type silicon, silicon nitride, ZnO thin film, source and drain electrodes. The ZnO thin film has an exposed channel of 70 μm long and 2000 μm wide for sensing various non-polar and polar solvents. The film is fabricated using a 0.05 M ZnO solution precursor which is synthesized by dissolving zinc acetate dihydrate $[\text{Zn}(\text{CH}_3\text{COO})_2 \cdot 2\text{H}_2\text{O}]$ into ethanol ($\text{CH}_3\text{CH}_2\text{OH}$, absolute $\geq 99.8\%$) and stirring for 2 h at 60 $^\circ\text{C}$.

Figure 1b shows the whole fabrication procedure of the TFT. First, a p-type silicon wafer doped heavily with boron (B) was treated via the standard Radio Corporation of America (RCA) cleaning process to remove metallic and organic contamination. Then, a 100-nm-thick silicon nitride (Si_3N_4) dielectric layer was deposited on the silicon substrate at 300 $^\circ\text{C}$ by plasma-enhanced chemical vapor deposition (PECVD). Subsequently, the ZnO precursor sol-gel solution was spin-coated on the silicon nitride dielectric layer. To form an active n-type semiconductor layer, spin-coating was carried out for 5 times at a maximum speed of 3000 rpm for 30 s, following an annealing process on a hot plate at 300 $^\circ\text{C}$ for 1 h. Finally, the bottom gate electrode was deposited on the back side of silicon wafer and the source and drain electrodes on the ZnO thin film by the thermal coating of 300-nm-thick aluminum (Al). A metal-mask of 70 μm long and 2000 μm wide was used during the deposition of source and drain electrodes to form an exposed channel on the thin film transistor.

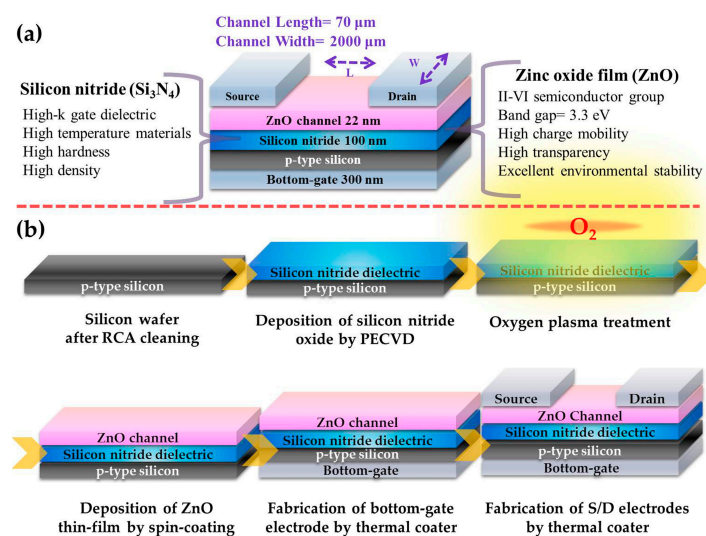


Figure 1. Zinc oxide (ZnO) based thin-film transistor (TFT) and its fabrication process. (a) Schematic diagram and illustration of ZnO-based TFT. For the TFT sensing, the ZnO film between two electrodes (source and drain electrodes, S/D) are exposed to various liquid solvents; (b) The fabrication procedure of a ZnO-based TFT by a low-temperature process.

3. Results and Discussion

3.1. Physical Analytics and Electrical Characterizations

Different techniques were used to characterize the ZnO-based TFTs. Figure 2a depicts a typical atomic force microscope (AFM) image of the ZnO thin film, indicating that the ZnO thin-film is continuous and smooth on the dielectric layer and the film roughness is less than 3 nm. Figure 2b shows the X-ray diffraction (XRD) pattern of the thermally annealed ZnO thin film. The major diffraction peak

located at approximately 34.5° can be indexed to 002 of ZnO. This means that the grains in ZnO thin film may be textured with their *c*-axes along the film normal. The chemical structure and composition of as-deposited ZnO thin films were examined using X-ray photoelectron spectroscopy (XPS). The XPS spectrum (Figure 2c) shows characteristic peaks at 1023.1 eV and 1048.9 eV, which correspond to Zn 2p_{3/2} and Zn 2p_{1/2}, respectively.

The electrical transport properties of the ZnO-based TFTs were investigated. Figure 2d shows the representative transfer characteristics of the devices in a dry environment, where the drain-source voltage (V_{DS}) varies from 0 to 40 V and bottom-gate bias voltage (V_{GS}) to the silicon substrate is in the range of 0 to 30 V at intervals of 5 V. The output drain-current (I_{DS}) is controlled by both V_{DS} and V_{GS} . These curves demonstrate saturation behavior of I_{DS} at high V_{DS} and saturation values of I_{DS} increase with V_{GS} .

The transfer characteristics of the ZnO-based TFT are shown in (Figure 2e, black curve, left scale). The source-drain current I_{DS} on a logarithmic scale varies with the gate voltage V_{GS} (from -20 to 30 V) at a constant V_{DS} of 5 V. When V_{GS} was at 30 V, the I_{DS} is about 1.12×10^{-5} A in logarithmic scale indicating that the on-off current (I_{ON} - I_{OFF}) ratio was approximately 10^6 . (Figure 2e, blue curve, right scale) presents the square root of I_{DS} saturation values ($I_{Drain,sat}$) vs. V_{GS} . From $I_{Drain,sat}$ vs. V_{GS} curves, the threshold voltage (V_{th}) of 2.75 ± 2.86 V for the Si₃N₄ dielectric layer and the field-effect mobility (μ_{FE}) of 0.0053 ± 0.0012 cm²·V⁻¹·s⁻¹ which were indicated by 0.0057, 0.0036, short circuit and 0.0065 can be determined according to the $I_{Drain,sat}$ Equation (1), and the other derived parameters are summarized in Table 1. The errors were calculated on the basis of measurements on 4 TFT devices. The TFT device is turned on by the electrons accumulated in the n-type ZnO channel layer when V_{GS} is in the positive voltage direction, so the device operates in an “n-channel semiconductor enhancement mode”. As indicated by the linear plot, the I_{ON} value measured when $V_{Gate} = 30$ V and $V_{Drain} = 5$ V was 3.3 mA. The solution-processed ZnO-based TFTs not only show excellent electrical characteristics, but also good stability.

The electrical stability of a ZnO-based TFT was investigated by measuring the I_{DS} - V_{GS} curves for 10 times on the same device, as shown in Figure 2f. The endurance test results of the TFT are repeatable and stable after 10 operations, so the TFT is suitable for sensing various liquid solvents.

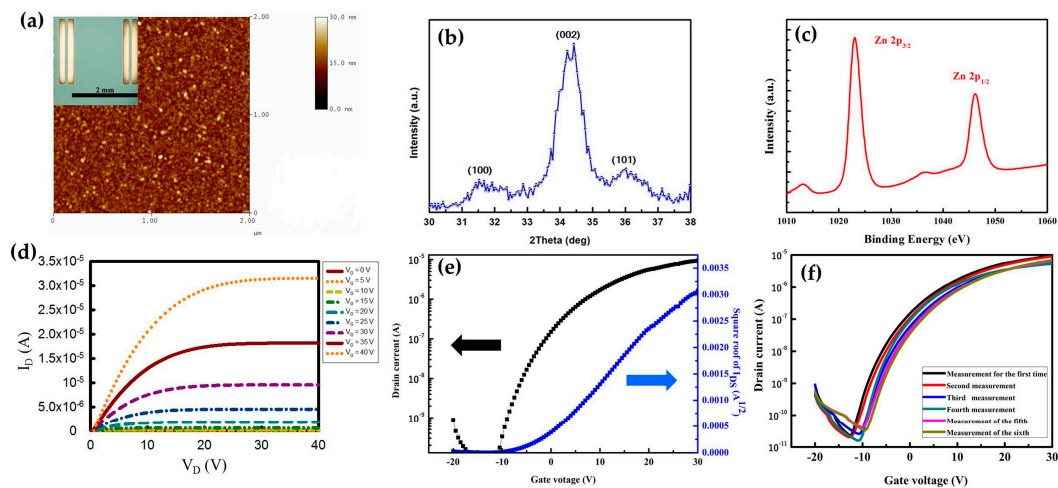


Figure 2. Physical analysis and electrical characterizations of ZnO-based TFTs in a dry environment: (a) Atomic force microscope (AFM) and the optical microscope (OM) image (inset) of the TFT; (b) X-ray diffraction (XRD) spectrum in the range of 30° – 38° ; (c) The X-ray photoelectron (XPS) spectrum of ZnO film showing Zn 2p peaks; (d–f) The electrical characterizations of the TFT; (d) I_{DS} - V_{DS} curves, drain current as a function of drain voltage with the bottom gate voltage ($V_{GS,bottom}$) varying from 0 to 40 V with steps of 5 V; (e) I_{DS} - V_{GS} , drain current versus bottom gate voltage ($V_{GS,bottom}$) varying from -20 to 30 V with steps of 500 mV, with the drain voltage being fixed at 5 V and the drain current being plotted on a logarithmic scale (left) and the square root of drain current plotted on a linear scale (right); (f) The endurance test for 10 iterations of I_{DS} - V_{GS} curves.

3.2. Specific Detection of Polar and Non-Polar Liquid Solvents

Liquid solvents can be generally divided into nonpolar molecule (e.g., toluene) and polar molecule (e.g., ethanol) categories because of high or low dielectric constants. In this section, we investigate the electrical effect of a nonpolar solvent (toluene), a polar solvent (ethanol) and water (deionized water) onto the exposed ZnO channel of the TFTs. All of the three solutions resulted in an immediate response of the TFT device when they were dropped onto the ZnO surface. Whether their electrical parameters gradually return to their initial states after solution degradations (drying) was also examined.

The I_{DS} - V_{GS} characteristics of the TFTs exposed to three liquids with different dielectric constant values are shown in Figure 3. Figure 3a shows the experimental diagram of the TFT device and liquid. All TFTs were operated in a saturated region with the V_{GS} varying from -25 to 25 V at a constant V_{DS} of 5 V. The “initial state”, shown in Figure 3b, means that the ZnO-based TFT device was not exposed to any solvents. When toluene was dropped onto the ZnO surface at 0 min, a threshold voltage (V_{th}) did not show any significant negative shift (Figure S1) and no field-effect mobility (μ_{FE}) degradation was observed. In contrast, the polar molecules were charged together on the interface of the ZnO film channel through the bottom-gate voltage, which determined the effective channel surface potential of the dielectric. From the drain current shown as the function of V_{GS} , we observed a significant increase in the drain current (Figure 3c) when ethanol was dropped on the ZnO channel. Meanwhile, the V_{th} was shifted to a negative direction by about -6 V (Figure S2). Ionized water caused electrical shorts (Figures 3d and S3) when it adsorbed on the ZnO channel at 0 min. toluene, ethanol and de-ionized water have dielectric constants of about 2.4 , 24 and 80 , respectively. The different response of the TFT to toluene, ethanol and de-ionized water may be related to their dielectric constants. The electrical parameters are summarized in Table 1. This V_{th} shift in the negative direction or electrical short was attributed to the extra electrons from the polar molecules accumulating on the ZnO channel due to their polarity or electronegativity. When the molecules are dropped and adsorbed on the exposed ZnO channel surface, a low V_{GS} operating voltage was required to turn on the TFT devices. Due to this phenomenon, the magnitudes of the V_{th} and V_{on} shifts depend on the dielectric constants of the solvents, leading to the successful demonstration of a solution-processed ZnO-based TFT solvent molecule sensing.

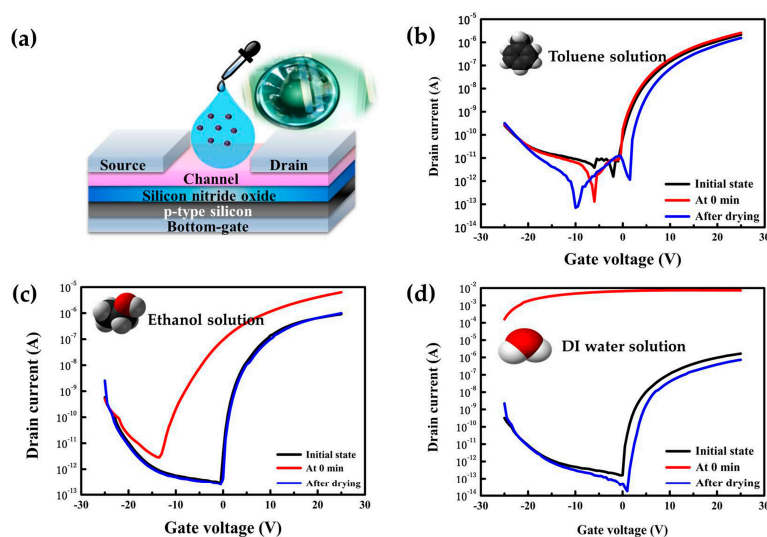


Figure 3. Transfer characteristics I_{DS} - V_{GS} of solution-processed ZnO-based TFT sensors for various polar and non-polar solvents and DI water. (a) Illustration of dropping various liquid solvents on the ZnO sensing area between two electrodes (S/D); (b) A non-polar liquid solvent of toluene with a dielectric constant value of approximately 2.4 ; (c) A polar liquid solvent of ethanol with a dielectric constant value of approximately 24 ; and (d) A DI water with high dielectric constant of approximately 80 , leading to a highly charged surface on the channel surface. The thickness of ZnO channel film used was approximately 22 nm prepared by the spin-coating shown in Figure S4.

Those V_{th} and V_{on} values were almost recovered to their initial states via drying process. In addition to being used as a liquid molecule sensor, this solution-processed ZnO-based TFT device is a potential candidate for utilization as a bio-sensor in which its reaction with liquid solvents in bio-materials may lead to additional carrier charge on the interface between the semiconductor channel and biomaterials. Table 1 summarizes the electrical parameters of solution-processed ZnO-based TFT devices such as μ_{FE} and V_{th} for different solvents at the initial state, 0 min after droplet application, and after drying with respect to the dielectric constant of each solvent.

Table 1. Comparison of the electrical parameters of the ZnO-based TFT sensor under different conditions such as initial state and the various solvents on the exposed ZnO channel.

Parameters	Dielectric Constant	$I_{ON/OFF}$	V_{th} (V)	μ_{FE} ($cm^2 \cdot V^{-1} \cdot s^{-1}$)	V_{th} (V)-After Drying
Initial state	-	$\sim 10^6$	2.75 ± 2.86	0.0053 ± 0.0012	-
Toluene	2.4	$\sim 10^7$	4	0.0082	5
Ethanol	24	$\sim 10^8$	-6	0.0014	1
DI water	80	Short circuit	Short circuit	Short circuit	5

Drain current saturation equation:

$$I_{Drain,sat} = (W/2L) \cdot C_i \cdot \mu_{FE} \cdot (V_{GS,bottom} - V_{th})^2 \quad (1)$$

where W is the channel width, L is the channel length, C_i is the gate oxide capacitance per unit area, and $C_i = (\epsilon_0 \cdot \epsilon_r) / \text{thickness}$ (F/m), $\epsilon_r: Si_3N_4 = 6 \sim 7$, μ_{FE} is the effective electron mobility.

4. Conclusions

In summary, we have demonstrated a solution-processed ZnO-based TFT sensor with a highly transparent semiconducting channel which is able to sense various polar and non-polar liquid solvents and DI water. The sensor is fabricated by a low-temperature (200–300 °C) processing technique. ZnO-based TFTs provide stable electrostatic operating voltages through bottom gate electrode control and a high I_{ON}/I_{OFF} switching characteristic of approximately 10^7 . The ZnO-based TFT sensors are of low cost and environmentally safe, which is imperative for electric device applications in biological sensing.

Supplementary Materials: The following are available online at www.mdpi.com/1996-1944/10/3/234/s1, Figure S1: Transfer characteristic of the square root of drain current plotted on a linear scale of solution-processed ZnO-based TFT sensors for a non-polar liquid solvent of toluene with a dielectric constant value of approximately 2.4, Figure S2: Transfer characteristic of the square root of drain current plotted on a linear scale of solution-processed ZnO-based TFT sensors for a polar liquid solvent of ethanol with a dielectric constant value of approximately 24, Figure S3: Transfer characteristic of the square root of drain current plotted on a linear scale of solution-processed ZnO-based TFT sensors for a DI water with high dielectric constant of approximately 80, leading to a highly charged surface on the channel surface, Figure S4: The thickness of ZnO channel film used was approximately 22 nm prepared by the spin-coating.

Acknowledgments: This work was supported by the Ministry of Science and Technology of Taiwan, under Contract Nos. MOST 105-2221-E-167-029. All process steps for device fabrication were carried out using the facility at National Nano device Laboratories, Hsinchu, Taiwan. The authors would like to extend appreciation to Yong-Jhen Wu for his help and assist in the experiments.

Author Contributions: Hsin-Chiang You and Cheng-Jyun Wang conceived and designed the experiments; Cheng-Jyun Wang performed the experiments; Cheng-Jyun Wang analyzed the data; Hsin-Chiang You contributed reagents/materials/analysis tools; Cheng-Jyun Wang wrote the paper.

Conflicts of Interest: The authors declare no conflict of interest.

References

- Gómez-Pozos, H.; Arredondo, E.J.L.; Álvarez, A.M.; Biswal, R.; Kudriavtsev, Y.; Pérez, J.V.; Casallas-Moreno, Y.L.; de la Luz Olvera Amador, M. Cu-Doped ZnO thin films deposited by a sol-gel process using two copper precursors: Gas-sensing performance in a propane atmosphere. *Materials* **2016**, *9*, 87. [[CrossRef](#)]

2. Dunkel, C.; Graberg, T.V.; Smarsly, B.M.; Oekermann, T.; Wark, M. Limits of ZnO electrodeposition in mesoporous tin doped indium oxide films in view of application in dye-sensitized solar cells. *Materials* **2014**, *7*, 3291–3304. [[CrossRef](#)]
3. Kolodziejczak-Radzimska, A.; Jesionowski, T. Zinc oxide—from synthesis to application: A review. *Materials* **2014**, *7*, 2833–2881. [[CrossRef](#)]
4. Tachikawa, S.; Noguchi, A.; Tsuge, T.; Hara, M.; Odawara, O.; Wada, H. Optical properties of ZnO nanoparticles capped with polymers. *Materials* **2011**, *4*, 1132–1143. [[CrossRef](#)]
5. Vuttipittayamongkol, P.; Wu, F.; Chen, H.; Cao, X.; Liu, B.; Zhou, C. Threshold voltage tuning and printed complementary transistors and inverters based on thin films of carbon nanotubes and indium zinc oxide. *Nano Res.* **2014**, *8*, 1159–1168. [[CrossRef](#)]
6. Kim, Y.H.; Heo, J.S.; Kim, T.H.; Park, S.; Yoon, M.H.; Kim, J.; Oh, M.S.; Yi, G.R.; Noh, Y.Y.; Park, S.K. Flexible metal-oxide devices made by room-temperature photochemical activation of sol–gel films. *Nature* **2012**, *489*, 128–132. [[CrossRef](#)] [[PubMed](#)]
7. Banger, K.K.; Yamashita, Y.; Mori, K.; Peterson, R.L.; Leedham, T.; Rickard, J.; Sirringhaus, H. Low-temperature, high-performance solution-processed metal oxide thin-film transistors formed by a “sol-gel on chip” process. *Nat. Mater.* **2011**, *10*, 45–50. [[CrossRef](#)] [[PubMed](#)]
8. Avis, C.; Hwang, H.R.; Jang, J. Effect of Channel Layer Thickness on the Performance of Indium-Zinc-Tin Oxide Thin Film Transistors Manufactured by Inkjet Printing. *ACS Appl. Mater. Interfaces* **2014**, *6*, 10941–10945. [[CrossRef](#)] [[PubMed](#)]
9. Cipriano, T.; Knotts, G.; Laudari, A.; Bianchi, R.C.; Alves, W.A.; Guha, S. Bioinspired peptide nanostructures for organic field-effect transistors. *ACS Appl. Mater. Interfaces* **2014**, *6*, 21408–21415. [[CrossRef](#)] [[PubMed](#)]
10. Zhang, W.; Patel, K.; Schexnider, A.; Banu, S.; Radadia, A.D. Nanostructuring of biosensing electrodes with nanodiamonds for antibody immobilization. *ACS Nano* **2014**, *8*, 1419–1428. [[CrossRef](#)]
11. Lin, P.; Yan, F.; Chan, H.L.W. Ion-sensitive properties of organic electrochemical transistors. *ACS Appl. Mater. Interfaces* **2010**, *2*, 1637–1641. [[CrossRef](#)] [[PubMed](#)]
12. Liu, N.; Liu, Y.; Zhu, L.; Shi, Y.; Wan, Q. Low-Cost pH Sensors Based on Low-Voltage Oxide-Based Electric-Double-Layer Thin Film Transistors. *IEEE Electron. Device Lett.* **2014**, *35*, 482–484. [[CrossRef](#)]
13. Zhang, Q.; Liu, W.; Sun, C.; Zhang, H.; Pang, W. On-chip surface modified nanostructured ZnO as functional pH sensors. *Nanotechnology* **2015**, *26*, 355202. [[CrossRef](#)] [[PubMed](#)]
14. Kumar, N.; Kumar, J.; Panda, S. Back-channel electrolyte-gated a-IGZO dual-gate thin-film transistor for enhancement of pH sensitivity over nernst limit. *IEEE Electron. Device Lett.* **2016**, *37*, 500–503. [[CrossRef](#)]
15. Sarkar, D.; Liu, W.; Xie, X.; Anselmo, A.C.; Mitragotri, S.; Banerjee, K. MoS₂ field-effect transistor for next-generation label-free biosensors. *ACS Nano* **2014**, *8*, 3992–4003. [[CrossRef](#)] [[PubMed](#)]
16. Lee, D.W.; Lee, J.; Sohn, I.Y.; Kim, B.Y.; Son, Y.M.; Bark, H.; Jung, J.; Choi, M.; Kim, T.H.; Lee, C.; et al. Field-effect transistor with a chemically synthesized MoS₂ sensing channel for label-free and highly sensitive electrical detection of DNA hybridization. *Nano Res.* **2015**, *8*, 2340–2350. [[CrossRef](#)]
17. Jung, J.; Kim, S.J.; Lee, K.W.; Yoon, D.H.; Kim, Y.g.; Kwak, H.Y.; Dugasani, S.R.; Park, S.H.; Kim, H.J. Approaches to label-free flexible DNA biosensors using low-temperature solution-processed InZnO thin-film transistors. *Biosens. Bioelectron.* **2014**, *55*, 99–105. [[CrossRef](#)] [[PubMed](#)]
18. Medina-Sánchez, M.; Martínez-Domingo, C.; Ramon, E.; Merkoçi, A. An inkjet-printed field-effect transistor for label-free biosensing. *Adv. Funct. Mater.* **2014**, *24*, 6291–6302. [[CrossRef](#)]

